

Macroscopic manifestations of rotating triaxial superfluid nuclei

P. Schuck^{1,2,*} and M. Urban^{1,†}

¹*Institut de Physique Nucléaire, CNRS-IN2P3, Univ. Paris-Sud,
Université Paris-Saclay, F-91406 Orsay Cedex, France*

²*Univ. Grenoble Alpes, CNRS, LPMMC, F-38000 Grenoble, France*

Recently, Allmond and Wood [Phys. Lett. B **767**, 226 (2017)] were able to extract the three moments of inertia \mathfrak{J}_k of a dozen of superfluid triaxial nuclei from experimental data. The observed dependence of the \mathfrak{J}_k on the deformation parameters is rather smooth. Here we show that these moments of inertia can be surprisingly well explained by a semiclassical cranked Hartree-Fock-Bogoliubov (HFB) calculation in which the velocity field is a simple superposition of rigid and irrotational flows.

I. INTRODUCTION

It is a well known fact that superfluidity has an important influence on nuclear rotation. This for instance induces a strong reduction of the moment of inertia of superfluid nuclei by factors two, three, or more.

In the past this feature was revealed in the great majority of cases for rotation of axially symmetric nuclei. Rotation of triaxially deformed nuclei is much scarcer and less well born out (see, e.g., Ref. [1] for an early work and Ref. [2] for one of the latest developments). Very recently, Allmond and Wood [3] made a very nice analysis of a dozen of the clearest triaxially deformed nuclei in deducing experimentally their moments of inertia around the three axes. In Fig. 1, we show a reproduction of their figure for the three moments of inertia corresponding to the three axes. Besides very few exceptions the experimental results (red crosses) lie with relatively little scatter around a straight line. This new and surprising feature calls for a simple explanation.

As early as in 1959, Migdal developed a statistical description of rotating superfluid nuclei where he applied some sort of Strutinsky smoothing of a superfluid contained in a deformed harmonic oscillator potential while making also some estimates how things would change with a hardwall box potential [4]. He was able to well explain the general trend of the superfluid quadrupole moment of inertia as a function of deformation and neutron number, see Fig. 1 in [4]. In 1985, Durand, Schuck, and Kunz [5] translated Migdal's statistical approach into a semiclassical transport model. The formulae for the moment of inertia stayed unchanged, only it was then possible to also calculate the current distributions. It was shown that the current distribution in rotating superfluid nuclei evolves as a function of the gap value from rigid rotation for small gaps to irrotational flow patterns for very large gaps. Realistic values of the gap show intermediate features of the flow.

From the late 90s, experimentalists achieved to pro-

duce atomic Bose-Einstein condensates in traps. Anticipating that it would become possible to trap also fermionic atoms and cool them down to superfluidity, Farine et al. used the theory originally developed for nuclei to compute the moment of inertia of atomic Fermi gases [6]. In 2003, we elaborated a more advanced semiclassical transport approach to rotating superfluid fermionic atoms including the temperature dependence [7]. Indeed, a few years later, the experiment of a rotating Fermi gas was realized by the Innsbruck group and the reduction of the moment of inertia below the superfluid critical temperature was observed [8].

Concerning now the measurements of the moments of inertia in triaxially deformed superfluid nuclei, we only had to reactivate our past calculations and adopt them to the triaxial deformation. As we will see, we get very good agreement with the experimental values. Since these results come from a semiclassical approach where shell effects are absent, the agreement between theory and experiment reveals a *macroscopic* behavior of triaxially deformed superfluid nuclei. This is, maybe, a somewhat surprising but nice finding for such a subtle feature as is triaxial rotation. For completeness let us repeat our analytic formulae which we will use in order to explain the measurements of the moments of inertia as well as those needed for the calculation of the flow patterns.

II. FORMALISM

As stated in the introduction, we repeat the harmonic oscillator model of Migdal, generalized to triaxiality as in [6]. The starting point is a cranked HFB calculation to which a semiclassical approximation is applied. The formulas are given in our earlier publications and for completeness repeated here. For example, the superfluid moment of inertia is given by

$$\mathfrak{J} = \mathfrak{J}_{\text{rigid}} \left(1 - \frac{8\omega_x^2\omega_y^2 G_+ G_-}{(\omega_x^2 + \omega_y^2)(\omega_+^2 G_+ + \omega_-^2 G_-)} \right), \quad (1)$$

where ω_k are the frequencies of the triaxially deformed harmonic oscillator potential and $\omega_{\pm} = \omega_y \pm \omega_x$, $\mathfrak{J}_{\text{rigid}}$ is the corresponding rigid-body moment of inertia, and the

*Electronic address: schuck@ipno.in2p3.fr

†Electronic address: urban@ipno.in2p3.fr

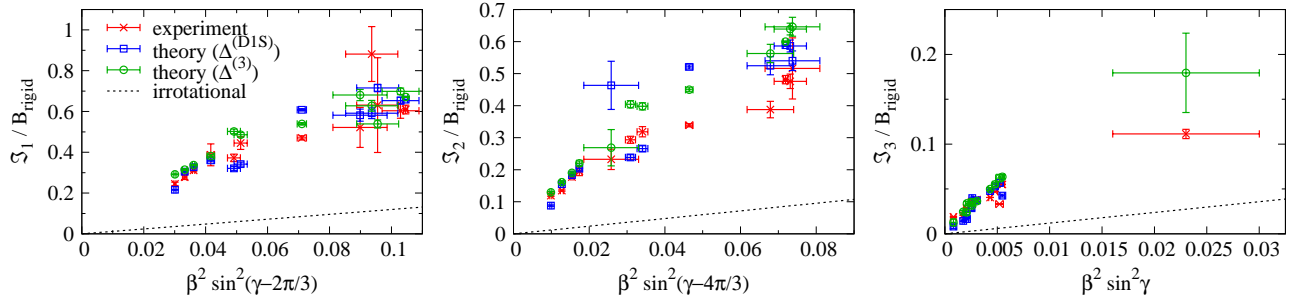


FIG. 1: Moments of inertia \mathcal{J}_k , plotted as a function of $\beta^2 \sin^2(\gamma - \frac{2\pi}{3}k)$ which is proportional to $\mathcal{J}_{k,\text{irrot}}$ (dashed line). The theoretical results were computed with the experimental deformation parameters β and γ [3] and the HFB pairing gaps $\Delta_{n,p}^{(\text{D1S})}$ [10] (blue boxes) and with the pairing gaps $\Delta_{n,p}^{(3)}$ from the 3-point formula (green circles). The error bars of the theoretical results include only the experimental uncertainties of β and γ . The results are compared with the experimental moments of inertia of Ref. [3] (red crosses).

functions G_{\pm} are given by

$$G_{\pm} = G\left(\frac{\hbar\omega_{\pm}}{2\Delta}\right), \quad (2)$$

where Δ is the gap at equilibrium at the Fermi level and

$$G(x) = \frac{\text{arcsinh}(x)}{x\sqrt{1+x^2}}. \quad (3)$$

From Eq. (1) one sees that in the limit of very strong pairing, $\Delta \gg \hbar\omega_i$ (i.e., $G_{\pm} \rightarrow 1$), the moment of inertia reduces to its irrotational value

$$\mathcal{J}_{\text{irrot}} = \left(\frac{\omega_x^2 - \omega_y^2}{\omega_x^2 + \omega_y^2}\right)^2 \mathcal{J}_{\text{rigid}}. \quad (4)$$

These formulas are arranged for a rotation around the z -axis, but rotation about the other two axes is easily achieved in permuting the axes.

The current corresponding to a rotation with angular velocity $\boldsymbol{\Omega} = \Omega \mathbf{e}_z$ is given by

$$\begin{aligned} \mathbf{j}(\mathbf{r}) &= \rho(\mathbf{r})\mathbf{v}(\mathbf{r}) \\ &= \Omega\rho(\mathbf{r})\left(r_x\mathbf{e}_y - r_y\mathbf{e}_x - \frac{4G_+G_-(\omega_x^2 r_x\mathbf{e}_y - \omega_y^2 r_y\mathbf{e}_x)}{\omega_+^2 G_+ + \omega_-^2 G_-}\right). \end{aligned} \quad (5)$$

Again, one sees that, with increasing gap, the velocity field changes continuously from the rigid rotation

$$\mathbf{v}_{\text{rigid}} = \boldsymbol{\Omega} \times \mathbf{r} \quad (6)$$

to the irrotational one

$$\mathbf{v}_{\text{irrot}} = \Omega \frac{\omega_y^2 - \omega_x^2}{\omega_y^2 + \omega_x^2} \nabla xy. \quad (7)$$

Equations (1) and (5) can be summarized in the compact form

$$\mathcal{J} = (1 - C)\mathcal{J}_{\text{rigid}} + C\mathcal{J}_{\text{irrot}}, \quad (8)$$

$$\mathbf{v} = (1 - C)\mathbf{v}_{\text{rigid}} + C\mathbf{v}_{\text{irrot}}, \quad (9)$$

$$C = \frac{2G_+G_-(\omega_x^2 + \omega_y^2)}{\omega_+^2 G_+ + \omega_-^2 G_-}. \quad (10)$$

III. RESULTS AND DISCUSSION

In order to produce numbers, we have to determine the parameters entering Eq. (8). The rigid-body moment of inertia for rotation about the k axis ($k = 1, 2, 3$ corresponding to x, y, z) is approximated as (see, e.g., [9])

$$\mathcal{J}_{k,\text{rigid}} = B_{\text{rigid}}\left(1 - \sqrt{\frac{5}{4\pi}}\beta \cos(\gamma - \frac{2\pi}{3}k)\right), \quad (11)$$

$$B_{\text{rigid}} = \frac{2}{5}mAR_0^2 = 0.0138A^{5/3}\hbar^2 \text{ MeV}^{-1}, \quad (12)$$

with m the nucleon mass, $R_0 = 1.2 \text{ fm } A^{1/3}$ the nuclear radius, and β and γ the deformation parameters (Hill-Wheeler coordinates). The oscillator frequencies ω_k are inversely proportional to the radii, i.e., up to corrections of higher order in β ,

$$\hbar\omega_k = 41 \text{ MeV } A^{-1/3}\left(1 - \sqrt{\frac{5}{4\pi}}\beta \cos(\gamma - \frac{2\pi}{3}k)\right). \quad (13)$$

To leading order in β , one thus obtains from Eq. (4)

$$\mathcal{J}_{k,\text{irrot}} = \frac{15}{4\pi}B_{\text{rigid}}\beta^2 \sin^2(\gamma - \frac{2\pi}{3}k). \quad (14)$$

In this work, we will consider the 12 triaxial nuclei whose β and γ values are listed in Table 1 of Ref. [3] [we corrected a typo in that table: for ^{110}Ru , the correct value is $\beta = 0.310(11)$ as can be inferred from the quadrupole moment Q_0 given in the same table].

We furthermore need the pairing gaps. The fact that neutron and proton gaps Δ_n and Δ_p are different can easily be accounted for by replacing [4]

$$\mathcal{J}(\Delta) \rightarrow \frac{N}{A}\mathcal{J}(\Delta_n) + \frac{Z}{A}\mathcal{J}(\Delta_p). \quad (15)$$

As explained in [6], what we need in our semiclassical approximation are the average gaps on the Fermi surface. They can be extracted, e.g., from HFB calculations with the D1S Gogny force [10] which describe the ground-state properties of these nuclei (including deformations) very well. More precisely, we denote by $\Delta_{n,p}^{(\text{D1S})}$ the HFB gaps

averaged with u^2v^2 as explained in Ref. [11]. An alternative and much simpler way to obtain values for the gaps is to compute them from the experimental nuclear masses M [12] using the 3-point formula

$$\Delta_n^{(3)} = \frac{1}{2}[M(N-1, Z) - 2M(N, Z) + M(N+1, Z)], \quad (16)$$

and analogously for $\Delta_p^{(3)}$. However, we are aware that in the case of even-even nuclei (which we are interested in), the results of this 3-point formula may be contaminated by mean-field effects. Nevertheless, as can be seen in Table I, the agreement with the HFB gaps is on the average not too bad.

In Fig. 1 we show the resulting moments of inertia \mathcal{J}_k of the 12 triaxial nuclei considered in [3], plotted as a function of the combination of deformation parameters $\beta^2 \sin^2(\gamma - \frac{2\pi}{3}k)$, which is proportional to $\mathcal{J}_{k,\text{irrot}}$, for the two choices of pairing gaps. To make the identification between points in the figures and nuclei easier, we have listed the values of $\beta^2 \sin^2(\gamma - \frac{2\pi}{3}k)$ for each nucleus in Table I. For each of the three axes $k = 1, 2, 3$, the moments of inertia lie more or less on a smooth curve between $\mathcal{J}_{k,\text{irrot}}$ and $\mathcal{J}_{k,\text{rigid}}$.

The overall agreement between theoretical (blue boxes and green circles) and experimental (red crosses) moments of inertia is surprisingly good. Of course there are some cases where it works less well, as expected for a semiclassical theory which does not include shell effects. With the HFB gaps $\Delta_{n,p}^{(\text{D1S})}$ (blue boxes), the agreement with experiment is not as good as with $\Delta_{n,p}^{(3)}$, but globally still satisfactory. In particular, there are some outliers, such as ^{110}Ru for which especially \mathcal{J}_2 and \mathcal{J}_3 are clearly too large. This can be traced back to the very small HFB gaps $\Delta_{n,p}^{(\text{D1S})}$ in this nucleus (see Table I).

It is interesting to see where, for a given nucleus, the difference in $\mathcal{J}_k/B_{\text{rigid}}$ depending on the axis k comes from. To answer this question, one can look at the velocity fields. As an example, we show in Fig. 2 the velocity fields computed for the nucleus ^{150}Nd for rotations about the three axes (the $\Delta_{n,p}^{(3)}$ pairing gaps were used in this example). As one can see, the velocity field is neither that of a rigid rotation nor purely irrotational. But in the case of the rotation about the x axis, the rotational component is clearly larger than in the case of the rotation about the z axis where the velocity field is closer to the typical form of irrotational flow. And since $\mathcal{J}_{\text{irrot}}$ is very small if the nucleus is almost symmetric with respect to the rotation axis, this explains why \mathcal{J}_3 is so much smaller than \mathcal{J}_1 . In the present example, our calculation gives $\mathcal{J}_1/\mathcal{J}_3 \simeq 17$ which is close to the ratio of the experimental moments of inertia $\mathcal{J}_1/\mathcal{J}_3 \simeq 14$.

IV. CONCLUSIONS

In this work, we calculated the three moments of inertia of triaxial superfluid nuclei as they were deduced experimentally in a recent paper by Allmond and Wood [3].

We used for that a semiclassical approach which we had developed earlier for rotating superfluid atomic clouds [6, 7] and which is actually based on a very early work of Migdal concerning rotating superfluid axially symmetric nuclei [4], see also [5]. In the case of cold atoms, a semiclassical approach seems very well justified since the number of atoms can reach around a million. In finite nuclei, expectation values of observables are often overshadowed by strong shell fluctuations and a semiclassical approach can only yield an average value. However, as the work by Allmond and Woods shows [3], apparently the moments of inertia \mathcal{J}_k exhibit a rather smooth behavior as a function of the variable $\beta^2 \sin^2(\gamma - \frac{2\pi}{3}k)$ (proportional to the moment of inertia in the case of purely irrotational flow) where β and γ are the Hill-Wheeler coordinates. So we used our analytic formulas given in [6] for the calculation of the three moments of inertia for each one of the 12 nuclei considered in [3]. To our surprise, the agreement with experiment can be judged as good to very good. Actually the experimental data show rather little shell fluctuations what hints to rotation of superfluid triaxial liquid drops. In this sense, a semiclassical description may be valid for quantal objects as small as nuclei. The moments of inertia lie half way in between rigid rotation and irrotational flow. To reproduce this feature is not trivial at all and confirms that triaxial nuclear rotation exhibits macroscopic aspects.

With our approach we were also able to calculate the flow patterns. Not surprisingly, we see a mixture of irrotational and rotational motion. Naturally the rotation around the axis with the least deformation shows the most pronounced irrotational behavior (and vice versa for the strongest deformation axis). It is very nice that analytic formulas are able to catch essentially all the subtle features of rotation of superfluid triaxial nuclei very well.

Acknowledgments

We are very grateful to S. Hilaire for providing us the HFB gaps $\Delta_{n,p}^{(\text{D1S})}$.

TABLE I: Values $\beta^2 \sin^2(\gamma - \frac{2\pi}{3}k)$ computed from β and γ given in [3], pairing gaps $\Delta_{n,p}^{(D1S)}$ computed with the D1S Gogny force [10], and $\Delta^{(3)}$ obtained from nuclear masses [12] using the 3-point formula, for the 12 triaxial nuclei considered in Ref. [3] and in the present paper.

Nucleus	$\beta^2 \sin^2(\gamma - \frac{2\pi}{3})$	$\beta^2 \sin^2(\gamma - \frac{4\pi}{3})$	$\beta^2 \sin^2 \gamma$	$\Delta_n^{(D1S)}$ (MeV)	$\Delta_p^{(D1S)}$ (MeV)	$\Delta_n^{(3)}$ (MeV)	$\Delta_p^{(3)}$ (MeV)
¹¹⁰ Ru	0.096(7)	0.025(8)	0.023(8)	0.82	1.10	1.31	1.78
¹⁵⁰ Nd	0.0711(16)	0.0464(10)	0.00261(8)	1.08	0.90	1.02	1.47
¹⁵⁶ Gd	0.093(9)	0.068(7)	0.0021(3)	1.39	1.08	1.09	1.24
¹⁶⁶ Er	0.1046(7)	0.0719(6)	0.00306(14)	0.92	1.49	1.02	1.20
¹⁶⁸ Er	0.103(6)	0.073(5)	0.00254(24)	1.09	1.18	0.88	1.21
¹⁷² Yb	0.090(9)	0.074(8)	0.0008(3)	1.25	1.17	0.83	1.21
¹⁸² W	0.0513(22)	0.0341(15)	0.00175(11)	1.20	2.01	0.95	1.12
¹⁸⁴ W	0.0491(22)	0.0309(14)	0.00210(15)	1.23	2.08	0.83	1.15
¹⁸⁶ Os	0.0417(13)	0.0174(8)	0.0052(4)	1.30	1.01	0.99	1.32
¹⁸⁸ Os	0.0361(4)	0.0155(3)	0.00432(14)	1.28	1.02	1.03	1.30
¹⁹⁰ Os	0.0332(8)	0.0128(4)	0.00479(24)	1.31	1.00	1.02	1.36
¹⁹² Os	0.0301(4)	0.0099(3)	0.00549(22)	1.44	1.45	0.99	1.44

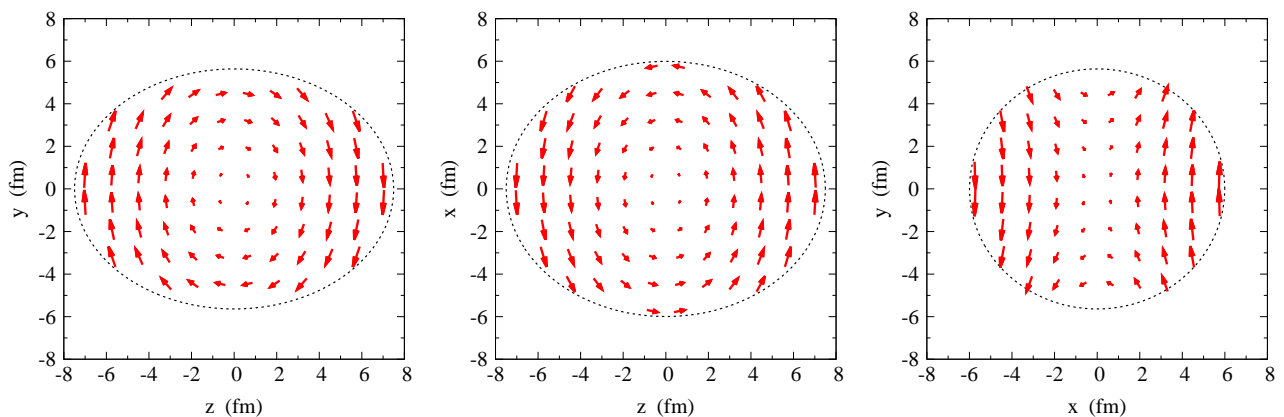


FIG. 2: Velocity fields in ¹⁵⁰Nd for rotations about the three principal axes. For better visibility, in the first two panels, the angular momentum is larger by a factor of two than in the third panel.

-
- [1] J. Helgesson and I. Hamamoto, Phys. Scr. **40**, 595 (1989).
[2] K. Washiyama and T. Nakatsukasa, JPS Conf. Proc. **23**, 013012 (2018).
[3] J. M. Allmond and J. L. Wood, Phys. Lett. B **767**, 226 (2017).
[4] A. B. Migdal, Nucl. Phys. **13**, 655 (1959).
[5] M. Durand, P. Schuck, and J. Kunz, Nucl. Phys. A **439**, 263 (1985).
[6] M. Farine, P. Schuck, and X. Viñas, Phys. Rev. A **62**, 013608 (2000).
[7] M. Urban and P. Schuck, Phys. Rev. A **67**, 033611 (2003).
[8] S. Riedl, E. R. Sánchez Guajardo, C. Kohstall, J. Hecker Denschlag, and R. Grimm, New J. Phys. **13**, 035003 (2011).
[9] P. Ring and P. Schuck, *The Nuclear Many-Body Problem* (Springer, New-York, 1980).
[10] S. Hilaire, private communication.
[11] S. Hilaire, J.-F. Berger, M. Girod, W. Satula, and P. Schuck, Phys. Lett. B **531**, 61 (2002).
[12] M. Wang, G. Audi, F. G. Kondev, W. J. Huang, S. Naimi, and X. Xu, Chinese Phys. C **41**, 030003 (2017).